materials

MDPI

Article

CFD-Based Evaluation of 3D-Printed Muffler Inserts: Impact of Internal Geometry on Pressure Drop and Turbulent Kinetic Energy

Tomáš Zvoníček [1], Libor Novák [1] and Petr Smolka [1,2] *

[1] Department of Physics and Materials Engineering, Faculty of Technology, Tomas Bata University in Zlín, Vavrečkova 5669, 760 01 Zlín, Czech Republic
[2] Centre of Polymer Systems, Tomas Bata University in Zlín, Třída Tomáš Bati 5678, 760 01 Zlín, Czech Republic
* Correspondence: smolka@utb.cz; Tel.: +420 576 035 110

Abstract

This study investigates the impact of internal muffler geometry on acoustic performance using steady-state Computational Fluid Dynamics (CFD) simulations. Four variants were analyzed: an empty tube, considered to be a baseline model, a three-chamber baffle system, a single spiral channel, and a complex multi-channel insert manufacturable only via advanced additive technologies. Simulations were conducted in SimScale using a compressible flow model with the k-ω SST turbulence formulation. Key outputs included static pressure distribution and turbulent kinetic energy (TKE), both of which are indirect indicators of acoustic attenuation. The results demonstrate that geometries incorporating spiral features significantly increase flow turbulence and pressure dissipation, suggesting enhanced damping potential. The study highlights how additive manufacturing enables the integration of acoustically favorable structures otherwise unattainable through conventional methods. By correlating pressure drop and TKE patterns with internal design features, the research offers a simulation-based framework for optimizing muffler performance in automotive exhaust systems. This approach provides an efficient alternative to experimental prototyping, supporting rapid evaluation and geometric refinement of sound-damping inserts

Keywords: Muffler design, Acoustic attenuation, Turbulent kinetic energy, Pressure drop, CFD simulation, Compressible flow, Additive manufacturing, 3D-printed inserts, Exhaust systems, Flow-induced noise

Academic Editor: Firstname Lastname

Received: date
Revised: date
Accepted: date
Published: date

Citation: To be added by editorial staff during production.

1. Introduction

In recent years, significant progress has been made in the use of complex internal structures and porous media for acoustic attenuation in confined systems such as silencers and mufflers. While experimental studies have traditionally focused on the measurement of sound absorption, reflectivity, or the mechanical-acoustic behavior of materials, increasing attention is now being paid to predictive modeling of acoustic performance using numerical methods. Among these, Computational Fluid Dynamics (CFD) has emerged as a robust tool for simulating compressible flows and sound propagation in intricate geometries, especially where direct experimentation is impractical or costly.

The internal configuration of silencers plays a critical role in determining acoustic efficiency. Studies such as Giedraitis and Kilikevicius have demonstrated how design modifications, particularly the use of multi-chambered configurations and smoothly varying cross-sections, can enhance acoustic attenuation by promoting energy dissipation [1]. Their findings are highly relevant to the implementation of 3D-printed inserts, which offer high design flexibility and can be tailored to specific flow and acoustic requirements.

Zeidan et al. explored the use of Tesla valves as passive flow control and damping elements. Their transient simulations showed that such geometries can effectively diffuse pressure spikes and redirect flow into vortical zones, thereby reducing the amplitude of pressure waves [2]. This confirms the potential of geometry-driven damping mechanisms, which can now be realized through additive manufacturing processes like SLM or DMLS.

Complementary research by Wurzinger et al. highlighted the importance of modeling not only acoustic pressure but also related properties such as impedance, wave speed, and resonance behavior in enclosed hydraulic systems prone to whistling or instability [3]. Their emphasis on time-domain resolution supports the idea that CFD-based acoustic analysis, especially under transient conditions, can provide deep insight into short-lived dynamic phenomena like shock waves or burst events.

Several investigations into automotive mufflers further reinforce the connection between internal baffle arrangement and overall system performance. Chandran demonstrated that the position and number of baffles significantly affect both sound suppression and pressure loss [4]. Rafique et al. examined extended chamber mufflers with micro-perforated panels and noted marked improvements in attenuation within the 500-2000 Hz range, without a proportional increase in backpressure [5]. Similarly, Liu et al. utilized time-dependent CFD to evaluate dissipative silencers under real exhaust flow and confirmed the predictive capability of such models in assessing both acoustic and aerodynamic performance [6].

These insights have been extended to 3D-printed muffler elements, including spiral chambers, periodic lattice structures, and multi-chambered designs. Simulation platforms like SimScale or COMSOL Multiphysics offer precise modeling of pressure fields, turbulence, and acoustic damping in real-world geometries. Notably, these tools allow comparative analysis of CNC-manufactured versus additively manufactured components, enabling developers to test more complex configurations without the need for costly prototypes [7].

Additive manufacturing further enables the fabrication of structures with features unattainable by conventional methods such as spiral baffles, gradient porosity, or internal periodic resonators. Technologies like SLS and DMLS facilitate the production of high-precision metal parts with defined acoustic properties [8].

From a physical perspective, sound attenuation in confined flow systems primarily occurs through two mechanisms: viscous dissipation, caused by velocity gradients near solid boundaries converting kinetic energy into heat, and thermal dissipation, resulting from cyclic compression and expansion of the fluid during acoustic wave propagation. These processes are especially relevant in muffler structures, where they contribute to broadband attenuation via local flow resistance and heat exchange. The Johnson-Champoux-Allard-Lafarge (JCAL) model provides a theoretical framework linking microstructural parameters, such as porosity, tortuosity, and characteristic lengths, to macroscopic acoustic performance and is widely used for modeling complex or additively manufactured porous media [9–12]. Structurally optimized materials with multiscale porosity extend the effective acoustic path length, enhancing both dissipation mechanisms. Periodic architectures like gyroid lattices allow frequency-selective damping and can be tuned through relative density, pore size, or wall thickness [13–16]. In spatially constrained environments such as automotive systems, these geometries enable acoustic tuning without altering macroscopic dimensions [17].

Within CFD modeling, two primary approaches to simulating acoustic damping have been established: (1) simplified interface-based models focusing on pressure drop and turbulence at structural boundaries, and (2) detailed simulations of internal porous domains or lattice-filled cavities. While the latter offers more granular insight into energy dissipation mechanisms, the former presents a more computationally feasible pathway for practical engineering applications [18,19].

In the context of this study, a simplified yet physically meaningful approach has been adopted. CFD simulations based on steady-state compressible flow were used to investigate four muffler configurations: a baseline empty exhaust tube, a three-chamber system with baffles, a single spiral channel insert, and a complex multi-channel geometry only realizable through 3D printing. The pressure distribution and turbulent kinetic energy (TKE) across these variants were analyzed to assess their potential for sound attenuation. The aim is to evaluate how geometric manipulation enabled by additive manufacturing can influence acoustic behavior, with CFD serving as a non-invasive tool for performance prediction [18,19].

To understand the impact of internal geometry on acoustic performance, it is essential to consider the mechanisms through which energy dissipation occurs in flow-acoustic systems. In particular, turbulent kinetic energy (TKE) and pressure distribution serve as important indicators of zones where acoustic energy may be converted into thermal energy, particularly through vortex shedding and flow recirculation [18,19].

CFD simulations, including those run in environments such as SimScale or COMSOL Multiphysics, enable the detailed analysis of such mechanisms across both conventional and additively manufactured designs. While direct modeling of acoustic wave propagation requires transient analysis or specific acoustic solvers, the pressure drop and TKE in steady-state compressible flows provide valuable insight into how structural design influences sound attenuation [18–20].

In more advanced modeling approaches, the internal structure of muffler inserts, such as gyroid infill, lattice frameworks, or micro-perforations can be explicitly resolved. These methods, while computationally demanding, yield detailed maps of flow-structure interaction and pressure fields, allowing identification of so-called acoustically active zones [17]. However, for practical design evaluation and optimization, simplified models that use pressure and TKE as surrogate markers for attenuation efficiency are both feasible and informative.

The choice between steady-state and transient analysis depends on the complexity of the acoustic phenomena under study. Steady-state models assume a temporally stabilized flow field and are typically employed for identifying pressure gradients, flow recirculation, and localized turbulence. Although they cannot resolve time-dependent wave phenomena, they are useful for comparative evaluation of muffler performance, particularly in early design stages [19].

In contrast, transient simulations are required to capture phenomena such as acoustic resonance, wave propagation, or short-duration pressure pulses. However, these simulations demand fine temporal resolution, stable numerical schemes, and significantly higher computational resources, especially for large or geometrically intricate domains [19].

Similarly, the decision between compressible and incompressible flow modeling hinges on the Mach number of the flow and the presence of significant density changes. In applications like exhaust silencers, where high-pressure gases and compressible flow behavior dominate, it is critical to model density variations to capture expansion, compression, and shock-related behavior accurately [21]. In such systems, only compressible models can reliably simulate the interaction between flow structures and acoustic damping effects.

Contemporary studies in the automotive sector demonstrate that optimizing internal muffler geometry through the addition of baffles, perforated layers, or porous inserts can significantly improve acoustic attenuation without compromising engine backpressure or exhaust flow [6,22]. Additive manufacturing enables the realization of such complex geometries, making it possible to integrate spiral channels, Helmholtz cavities, and structurally graded porosity into compact muffler units [8].

By combining CFD-based flow analysis with the geometric flexibility of 3D printing, this research contributes to a deeper understanding of how internal structure affects pressure fields and turbulence, and how these in turn relate to sound attenuation in confined exhaust systems. The ultimate goal is to support the design of more acoustically efficient, compact, and manufacturable muffler solutions using additive techniques.

Although this study does not directly simulate acoustic wave propagation, it aligns with established approaches that use pressure gradients and turbulent kinetic energy as surrogate markers for acoustic attenuation. These parameters provide physically meaningful indicators of energy dissipation via vortex shedding and flow instabilities—mechanisms that underpin effective sound damping in confined systems. By focusing on steady-state compressible CFD analysis, the present work offers a computationally efficient yet insightful method for evaluating how internal geometry influences acoustic behavior in additively manufactured mufflers.

2. Materials and Methods

2.1. Simulation environment and approach

The simulations were conducted using the cloud-based platform SimScale (https://www.simscale.com), applying a steady-state compressible flow model. This approach was selected to evaluate pressure distribution and turbulent kinetic energy (TKE) within the muffler geometry, with the aim of identifying potential zones of acoustic dissipation while maintaining reasonable computational cost.

The turbulence model applied was the k-ω SST (Shear Stress Transport), known for its ability to accurately predict near-wall behavior and separation under adverse pressure gradients. Although this method does not capture transient acoustic wave propagation, it provides relevant indicators such as pressure drop and TKE, which correlate with acoustic attenuation in internal flow systems [18,19].

2.2. Geometry and design variants

Four muffler configurations were analyzed:

Figure 1 presents the CAD models of the four muffler configurations evaluated in this study. These geometries were designed to isolate and compare the influence of internal flow-guiding structures on pressure distribution and turbulent kinetic energy (TKE) within the muffler body.

(A) Baseline (smooth pipe, no insert): The baseline model consists of a simple hollow cylindrical muffler with no internal structures or flow obstructions. It represents a straight-through exhaust design, providing an unimpeded flow path. This configuration serves as the control case for evaluating the impact of added geometrical complexity.

(B) Three-chamber baffle system: This variant incorporates two internal baffles, dividing the muffler into three chambers. The baffles are intended to partially redirect the flow and disrupt its coherence, thereby increasing turbulence levels and promoting energy dissipation through simple geometrical intervention.

(C) Single spiral insert: The third configuration introduces a spiral-shaped internal structure embedded within the cylindrical muffler. The spiral guides the airflow along a curved path, increasing the flow length and introducing rotational components to enhance turbulent mixing while preserving a centralized flow channel.

(D) Multi-channel 3D-printed insert: The final geometry features a highly complex internal structure composed of six curved channels that twist around the central axis of the muffler. This design, enabled by additive manufacturing, extends the effective flow path by inducing a helical trajectory. The objective is to generate controlled turbulence and maximize acoustic damping through geometric intricacy.

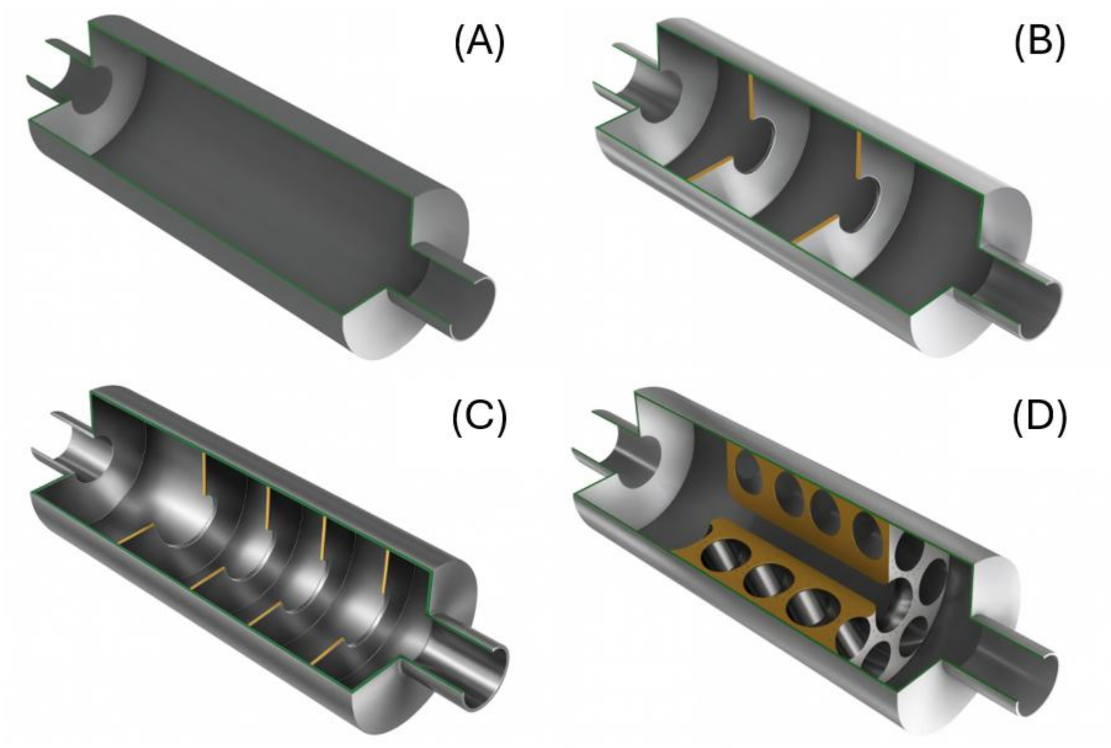

Figure 1. CAD models of for all four muffler configurations obtained from steady-state compressible CFD analysis. (A) Reference variant, (B) Three-chamber configuration with internal baffles, (C) Spiral insert, (D) Twisted multi-channel insert.

All variants were housed within the same external muffler casing geometry based on a real automotive silencer design.

2.3. Material modeling, boundary conditions and fluid parameters

In all CFD simulations, the muffler walls and internal inserts were modeled as rigid, adiabatic, and non-deformable surfaces. No fluid-structure interaction or vibroacoustic coupling was included. The aim was to isolate the effects of internal geometry on pressure distribution and turbulent kinetic energy, under the assumption that all configurations are constructed from the same solid material with sufficiently high stiffness (e.g., stainless steel or aluminum alloy). While this approach neglects potential contributions of structural damping or wall compliance to sound attenuation, it is commonly applied in steady-state flow-based acoustic analyses to maintain computational feasibility. Future work could extend the model to incorporate material-dependent boundary responses or multi-physics simulations involving structural dynamics.

The inlet boundary condition was defined as a pressure inlet of 0.14 MPa at 300 K, while the outlet was set to atmospheric pressure (0.101 MPa). Air was used as the working fluid, modeled as a compressible gas with ideal gas behavior.

- Inlet: Total pressure = 0.14 MPa
- Outlet: Static pressure = 0.101 MPa
- Temperature: 300 K
- Walls: No-slip boundary condition

2.4. Mesh and Solver Settings

Each geometry was discretized using automatically generated hexahedral-dominant meshes in SimScale with local refinement in zones of high expected velocity gradients (e.g., narrow channels and baffle regions). Mesh independence was verified by testing multiple refinement levels and confirming convergence of pressure drop and TKE results.

The solver applied compressible Navier-Stokes equations under steady-state assumptions. Residual convergence criteria were set to 1×10^{-4} for continuity and momentum equations, and all simulations were run until stable residual behavior was achieved.

2.5. Output Parameters

Primary simulation outputs included:

- Cross-sectional maps of pressure fields
- Cross-sectional maps of turbulent kinetic energy
- Line plots of pressure vs length for all four configurations

These metrics were selected to evaluate the flow-induced mechanisms relevant to acoustic attenuation, particularly the energy dissipation associated with internal vortex structures.

3. Results

The following section presents the outcomes of the CFD simulations, focusing on the effects of internal muffler geometry on pressure distribution and turbulent kinetic energy (TKE) across the four design variants.

3.1. Pressure Field Distribution

Figure 2 presents the distribution of static pressure within all four muffler variants obtained from the CFD analysis. The color scale indicates static pressure in kilopascals, with red regions representing high-pressure zones and blue corresponding to low-pressure areas near the outlet.

(A) Baseline geometry:

The baseline configuration is a straight cylindrical muffler without internal structures, exhibits an almost linear pressure decrease along its length. The main pressure drop occurs directly before the outlet, where the gas expands into the surrounding volume. The internal gradient is smooth and uniform, showing minimal energy losses or turbulence generation. This behavior confirms that a free, unobstructed flow path ensures low hydraulic resistance but provides little potential for acoustic attenuation.

(B) Three-chamber baffle system:

In contrast to the reference model, the baffles introduce a stepwise pressure reduction across the three chambers. Each partition induces localized losses that slow the flow and redistribute static pressure, as evident from the more gradual color transition from red to green-blue hues. The resulting pressure dissipation supports the reduction of flow coherence and, consequently, the attenuation of pressure-wave amplitude, which is desirable for noise control.

(C) Single spiral insert:

The spiral geometry produces a controlled combination of resistance and guided flow. The pressure decreases smoothly along the helical path without sharp discontinuities or back-flow regions. The color gradient is evenly distributed, indicating a balanced pressure field and efficient flow stabilization. The outlet pressure approaches values slightly above atmospheric (≈ 102 kPa), confirming that the spiral structure enables gradual energy dissipation while maintaining uniform flow which is an advantageous feature for acoustic damping with minimal flow penalty.

(D) Multi-channel 3D-printed insert:

The most complex configuration, composed of six curved channels twisting around the central axis, achieves the most homogeneous pressure field among all variants. The inlet zone (left) shows a high-pressure region near 140 kPa, which gradually decreases along the length of the muffler. The color transition from red-orange to green-blue demonstrates a continuous and evenly distributed pressure drop without abrupt transitions. The mid-section reveals redistribution of the pressure field across multiple sub-channels, leading to enhanced spatial uniformity both axially and radially. At the outlet (right), the pressure approaches 100-102 kPa, close to atmospheric levels, without noticeable gradients or reflection zones. This confirms that the additively manufactured multi-channel design enables highly efficient pressure management and flow homogenization, providing the best balance between flow continuity, controlled pressure reduction, and potential acoustic energy dissipation.

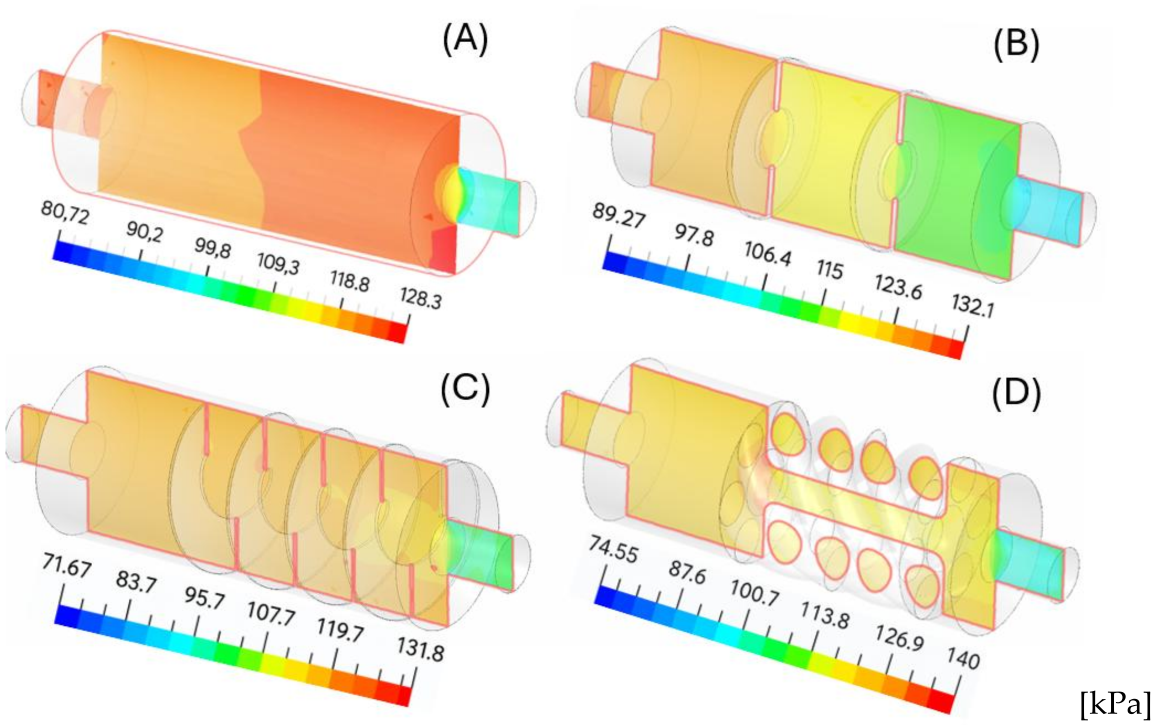

Figure 2. Static pressure distribution in kPa for all four muffler configurations obtained from steady-state compressible CFD analysis. (A) Baseline variant, (B) Three-chamber system with internal baffles, (C) Single spiral insert, (D) Multi-channel 3D insert. Note: Each image uses an individually scaled color bar to highlight internal pressure variations specific to the individual configuration.

3.2. Turbulent Kinetic Energy Distribution

Figure 3 shows the distribution of turbulent kinetic energy (TKE) within the four muffler configurations. The values, in units of m^2/s^2, are visualized on a logarithmic color scale, highlighting localized turbulence intensity throughout each geometry.

(A) Baseline:

The TKE distribution in the baseline configuration is concentrated near the inlet and especially the outlet zones, where flow accelerates sharply and interacts with ambient conditions. The central volume of the muffler remains largely unaffected, with turbulence levels significantly lower across most of the domain. The maximum recorded value reaches approximately 1637 m^2/s^2, confirming that in the absence of internal flow interruptions, the flow remains mostly laminar. This low-turbulence profile suggests limited potential for acoustic attenuation and energy dissipation.

(B) Three-chamber baffle system:

Compared to the reference model, this configuration demonstrates clearly elevated turbulence levels. Notable TKE intensities are observed between the internal baffles, particularly in the central region, with peak values approaching 1010 m^2/s^2. These localized zones of enhanced turbulence result from flow redirection and separation caused by the baffles. This increased turbulence is beneficial for scattering acoustic energy and breaking up coherent waveforms, contributing to more effective attenuation. The results confirm that even relatively simple baffle geometries can induce meaningful changes in flow structure, supporting their use in noise control applications. Furthermore, such designs are easily manufacturable using additive technologies.

(C) Spiral insert:

The TKE field in the spiral configuration reveals a more complex and spatially distributed turbulence pattern. The highest concentrations occur near the outlet and in the mid-sections of the spiral, where curvature and directional changes amplify vortex formation. Transitional zones between spiral turns exhibit moderate turbulence levels due to flow turning and shear interactions. In contrast, the core flow within the spiral channel remains relatively stable, with blue to green color zones indicating lower turbulence. The maximum TKE reaches around 773 m^2/s^2. This distribution suggests that the spiral insert offers a well-balanced combination of controlled turbulence which is important for acoustic damping and smooth flow behavior that avoids excessive resistance or flow separation.

(D) Multi-channel 3D-printed insert:

The most geometrically complex design exhibits the lowest overall turbulence intensity among the four configurations. The TKE ranges from approximately 2×10^{-8} to 548 m^2/s^2, with most of the internal domain dominated by low-to-moderate values (blue and light blue zones). Higher turbulence appears only in the inlet and outlet transition regions, where the flow enters or exits the structured domain. Inside the central volume, the multiple curved channels effectively suppress vortex formation, allowing the flow to redistribute gradually across the domain. The absence of high TKE peaks confirms that this geometry promotes laminarization and minimizes dynamic load fluctuations. This flow behavior is ideal not only for reducing noise but also for limiting structural fatigue and flow resistance making this configuration highly attractive for advanced muffler applications.

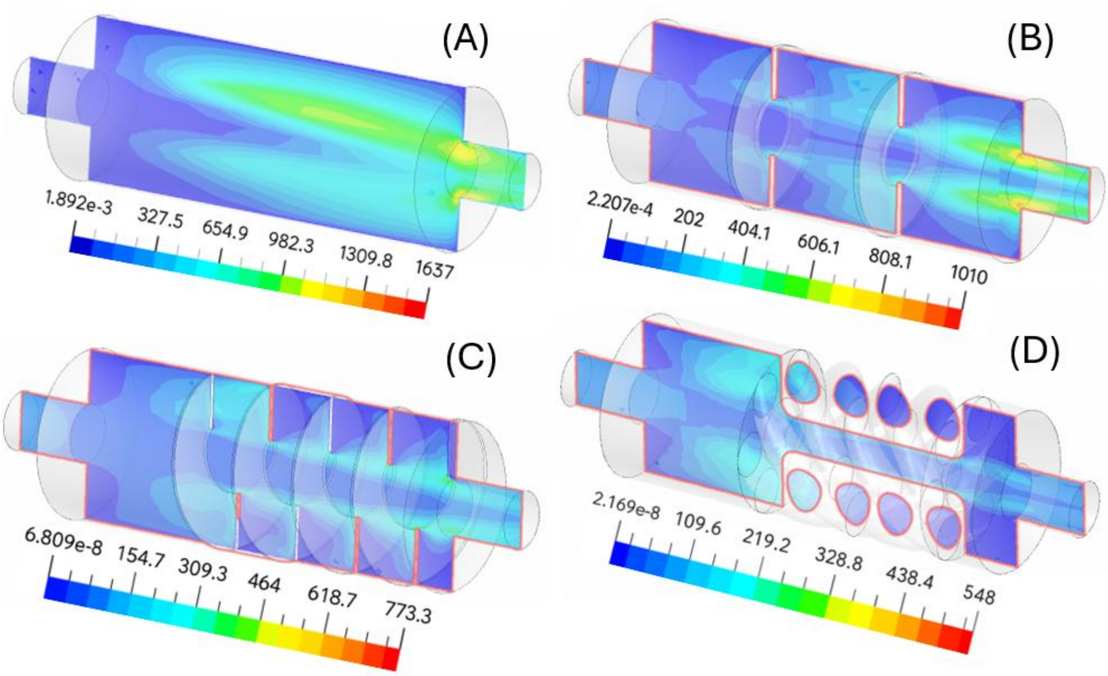

Figure 3. Turbulent kinetic energy in m^2s^2 for all four muffler configurations obtained from steady-state compressible CFD analysis. (A) Baseline variant, (B) Three-chamber system with internal baffles, (C) Single spiral insert, (D) Multi-channel 3D insert. Note: Each image uses an individually scaled color bar to highlight internal pressure variations specific to the individual configuration.

3.3. Pressure drop along the central axis

Figure 4 presents the pressure distribution along the muffler length for all four design variants, as extracted from the CFD simulations. The pressure was evaluated at a central axis probe spanning the full axial length (0-375 mm). These profiles allow direct comparison of flow resistance and internal energy dissipation across the different geometries.

(A) Baseline geometry:

The baseline configuration exhibits a gradual pressure decline from approximately 131 kPa at the inlet to ~102 kPa at the outlet. The central segment (~50-200 mm) shows a relatively flat pressure plateau, indicating minimal flow resistance and lack of energy dissipation. The sharp drop near the outlet reflects expansion into the ambient environment. This profile corresponds to unmodulated flow and minimal acoustic or hydraulic resistance.

(B) Three-chamber baffle system:

The baffle-based design exhibits a more nonlinear pressure trend. An initial slow decrease is followed by a steeper drop between 100-200 mm, associated with flow separation behind the internal partitions. This results in earlier and more distributed pressure loss. Peak inlet pressure reaches ~134 kPa, the highest of all cases, likely due to local compression near the baffles. This configuration demonstrates stronger flow modulation and pressure redistribution than the reference.

(C) Single spiral insert:

The spiral-guided variant shows a smooth, continuous pressure decay from ~134.4 kPa to ~102 kPa. The curved geometry creates a gradual pressure gradient with no sudden drops or stagnation points. The mid-section curve inflection indicates efficient control of velocity reduction and energy dissipation. This geometry balances resistance and flow continuity effectively, enhancing acoustic potential while minimizing backpressure peaks.

(D) Multi-channel 3D-printed insert:

The most complex design, featuring spatially twisted channels, achieves the smoothest and most uniform pressure gradient. The inlet pressure (~134.4 kPa) decreases steadily to ~102.8 kPa at the outlet, with no sharp transitions. This profile reflects exceptional control over flow dispersion and energy management, enabled by the additively manufactured domain. The curve suggests highly uniform energy dissipation and optimized acoustic behavior with minimal turbulence generation.

Overall, the comparison highlights a clear trend: as internal geometry complexity increases, the pressure profile becomes smoother and more evenly distributed, suggesting improved flow control and greater potential for acoustic attenuation. While the outlet pressures converge across all designs, the rate and uniformity of pressure decline differentiate the configurations. The multi-channel 3D geometry demonstrates the most technically desirable characteristics, combining smooth pressure decay with distributed resistance which are attributes critical for efficient, low-noise muffler performance.

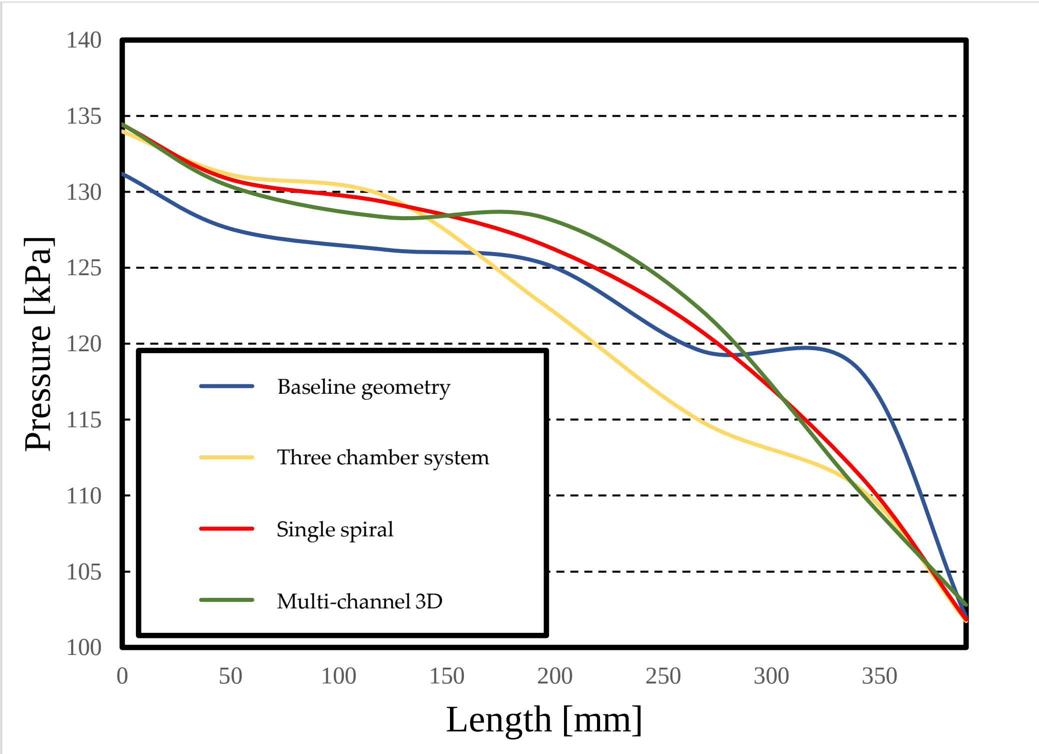

Figure 4. Pressure drop along the central axis of the muffler

4. Discussion

The results of the numerical simulations clearly demonstrate that the internal geometry of the muffler plays a critical role not only in shaping the static pressure distribution but also in influencing the flow behavior and turbulence intensity—factors that directly affect the acoustic performance of the device.

The reference baseline configuration, featuring a smooth, unobstructed internal geometry, exhibited the least interference with the flow field. The pressure drop occurred almost linearly along the muffler length, with the main pressure gradient appearing just before the outlet. Low turbulence levels within the muffler body indicated predominantly laminar flow, which, while beneficial for minimizing hydraulic resistance, resulted in limited potential for acoustic attenuation. These findings align with established theory, which suggests that smooth flow without acoustic obstacles fails to effectively dissipate acoustic energy.

The baffle-based three chamber configuration, comprising two partitions forming a three-chamber structure, marked a significant improvement in controlling flow-induced acoustic effects. The presence of internal partitions introduced localized pressure drops, particularly within the central chamber. The simulation of turbulent kinetic energy revealed the formation of targeted turbulence zones downstream of the baffles, which contributed to enhanced energy dissipation. This supports the theoretical understanding that even simple structural interventions can promote effective acoustic damping.

A substantial shift in attenuation behavior was observed in the single spiral configuration, enabled by additive manufacturing. The spiral channel forced the flow along an extended path, resulting in a smoother and more evenly distributed pressure drop. The pressure gradient was more gradual, indicating improved flow control. Turbulence visualizations showed that the spiral effectively generated focused turbulence, especially near the outlet and transitional zones, while maintaining relative stability in the central domain. This hybrid profile is a stable core flow combined with localized turbulence which is advantageous for achieving acoustic damping without excessive backpressure.

The most optimized flow and acoustic performance was achieved with the complex multi-spiral domain, fabricated exclusively through 3D printing. The intricate network of organically shaped channels enabled uniform pressure distribution and strategically placed turbulence. The pressure dropped smoothly across the entire structure, approaching atmospheric conditions at the outlet without abrupt changes. The TKE distribution showed that turbulence was concentrated only in critical transitional zones and effectively attenuated within the rest of the domain. The absence of high-turbulence pockets confirmed this geometry's ability to maintain uniform flow and minimize dynamic load—key factors for both acoustic and mechanical efficiency.

A comparative evaluation of all configurations indicates a clear trend: increasing geometric complexity leads to improved pressure control, redistribution of turbulent energy, and consequently enhanced acoustic damping. While the smooth reference design offered optimal flow characteristics, it lacked acoustic effectiveness. In contrast, baffle-based and spiral designs demonstrated that even basic geometrical modifications can significantly influence flow behavior. However, the 3D-printed domain variant exhibited the greatest potential, fully leveraging additive manufacturing capabilities for internal geometry optimization. This approach enables the design of multidimensional flow paths that balance pressure and turbulence - crucial for developing the next generation of compact, quiet, and efficient exhaust mufflers.

Future work may extend the current CFD-based approach by incorporating equivalent fluid models, such as the Johnson-Champoux-Allard-Lafarge framework, to simulate the acoustic behavior of porous or complex structures with reduced computational cost. This would enable direct calculation of transmission loss and acoustic impedance in conjunction with structural optimization.

Author Contributions: Conceptualization, T.Z. and P.S.; data curation, T.Z.; formal analysis, T.Z., L.N. and P.S.; investigation, T.Z.; methodology, T.Z., L.N. and P.S.; validation, P.S.; writing—original draft, T.Z., and P.S. All authors have read and agreed to the published version of the manuscript.

Funding: This publication was created as part of the implementation of the project Testing laboratory for the implementation of sustainable and resilient technologies, reg. number CZ.02.01.01/00/23_021/0010411, co-financed by the European Union under the OP Jan Amos Comenius. The author Petr Smolka thanks the project DKRVO (RP/CPS/2024-2028/003) too. The author Tomáš Zvoníček thanks the TBU Grant No. IGA/FT/2024/007 and IGA/FT/2025/005.

Acknowledgments: The authors would like to express their gratitude to the SimScale platform (https://www.simscale.com) for the access to the simulation tools.

Conflicts of Interest: The authors declare no conflict of interest.

References

1. GIEDRAITIS, V.; KILIKEVIČIUS, A. Performance Analysis of Different Firearm Suppressor Structures. *Mechanics* **2024**, *30*, 57–65, doi:10.5755/j02.mech.35196.
2. Zeidan, M.; Németh, M.; Abhijith, G.R.; Wéber, R.; Ostfeld, A. Transient Flow Dynamics in Tesla Valve Configurations: Insights from Computational Fluid Dynamics Simulations. *Water (Basel)* **2024**, *16*, 3492, doi:10.3390/w16233492.

3. Wurzinger, A.; Schoder, S.; Mayr-Mittermüller, B.; Kaltenbacher, M.; Sima, H. Hydrodynamic and Flow-Acoustic Simulation of a Two-Chamber Piston Hydraulic System Prone to Whistling. *Results in Engineering* **2025**, *26*, 105220, doi:10.1016/j.rineng.2025.105220.
4. C., M.R. Analysis of Various Automotive Mufflers: Computational Fluid Dynamics Approach. *Revista Gestão Inovação e Tecnologias* **2021**, *11*, 1339–1348, doi:10.47059/revistageintec.v11i4.2191.
5. Rafique, F.; Hui Wu, J.; Rui Liu, C.; Ma, F. Transmission Loss Analysis of a Simple Expansion Chamber Muffler with Extended Inlet and Outlet Combined with Inhomogeneous Micro-Perforated Panel (IMPP). *Applied Acoustics* **2022**, *194*, 108808, doi:10.1016/J.APACOUST.2022.108808.
6. Liu, L.; Zheng, X.; Hao, Z.; Qiu, Y. A Time-Domain Simulation Method to Predict Insertion Loss of a Dissipative Muffler with Exhaust Flow. *Physics of Fluids* **2021**, *33*, doi:10.1063/5.0056316.
7. İnan, A.T.; Köten, H.; Kartal, M.A. Experimental Comparison and CFD Analysis of Conventional Shell and Tube Heat Exchanger with New Design Geometry at Different Baffle Intervals. *Numeri Heat Transf A Appl* **2023**, *83*, 522–533, doi:10.1080/10407782.2022.2101801.
8. Zhuravlev, E.; Chugunkov, D.; Seyfelmlyukova, G. Improving the Acoustic Efficiency of Laminated Dissipative Noise Silencers for Boiler Gas-Air Paths. *E3S Web of Conferences* **2019**, *140*, 02005, doi:10.1051/e3sconf/201914002005.
9. Allard, J.F.; Atalla, N. *Propagation of Sound in Porous Media*; Wiley, 2009; ISBN 9780470746615.
10. Di Giulio, E.; Perrot, C.; Dragonetti, R. Experimental Characterization of Thermal and Viscous Powers in Porous Media under Oscillating Flow. *Thermal Science and Engineering Progress* **2024**, *56*, 103057, doi:10.1016/J.TSEP.2024.103057.
11. Jaouen, L.; Bécot, F.-X.; Chevillotte, F. Characterizations of Acoustical Porous Media: Standardized Methods, Current Trends and Challenges. *Frontiers in Acoustics* **2025**, *3*, doi:10.3389/facou.2025.1543456.
12. Yang, D.; Jiang, Q.; Wu, J.; Han, Y.; Ding, B.; Niu, B.; Xie, G. Acoustic Slow-Wave Effect Metamaterial Muffler for Noise Control of HVDC Converter Station. *Front Mater* **2022**, *8*, doi:10.3389/fmats.2021.804302.
13. Van Damme, B.; Cavalieri, T.; Nguyen, C.-T.; Perrot, C. Enhancement of the Sound Absorption of Closed-Cell Mineral Foams by Perforations: Manufacturing Process and Model-Supported Adaptation. *Mater Des* **2025**, *249*, 113540, doi:10.1016/j.matdes.2024.113540.
14. Nsiempba, K.M.; Wang, M.; Vlasea, M. Geometrical Degrees of Freedom for Cellular Structures Generation: A New Classification Paradigm. *Applied Sciences* **2021**, *11*, 3845, doi:10.3390/app11093845.
15. Guan, X.; Yang, J.; Deckers, E.; Hornikx, M. Computational Characterization of Functionally Graded Porous Absorbers Based on Triply Periodic Minimal Surfaces (TPMS). In Proceedings of the Proceedings of the 10th Convention of the European Acoustics Association Forum Acusticum 2023; European Acoustics Association: Turin, Italy, January 17 2024; pp. 4939–4946.
16. Zhang, M.; Liu, C.; Deng, M.; Li, Y.; Li, J.; Wang, D. Graded Minimal Surface Structures with High Specific Strength for Broadband Sound Absorption Produced by Laser Powder Bed Fusion. *Coatings* **2023**, *13*, 1950, doi:10.3390/coatings13111950.
17. Li, X.; Chua, J.W.; Yu, X.; Li, Z.; Zhao, M.; Wang, Z.; Zhai, W. 3D-Printed Lattice Structures for Sound Absorption: Current Progress, Mechanisms and Models, Structural-Property Relationships, and Future Outlook. *Advanced Science* **2024**, *11*, doi:10.1002/advs.202305232.
18. Elsayed, A.; Bastien, C.; Medina, H.; Jones, S.; Kassem, H. Enhancing Noise Attenuation in Exhaust Mufflers on Response to Baffle Configuration. *International Journal of Engineering and Manufacturing* **2017**, *7*, 12–25, doi:10.5815/ijem.2017.04.02.
19. Nouhaila, O.; Hassane, M.; Scutaru, M.L.; Jelenschi, L. On the Accuracy of Turbulence Model Simulations of the Exhaust Manifold. *Applied Sciences* **2024**, *14*, 5262, doi:10.3390/app14125262.

20. Zhang, H.; Fan, W.; Guo, L.-X. A CFD Results-Based Approach to Investigating Acoustic Attenuation Performance and Pressure Loss of Car Perforated Tube Silencers. *Applied Sciences* **2018**, *8*, 545, doi:10.3390/app8040545.
21. Tan, L.; Yuan, Y.; Tang, L.; Huang, C. Numerical Simulation on Fluid Flow and Temperature Prediction of Motorcycles Based on CFD. *Alexandria Engineering Journal* **2022**, *61*, 12943–12963, doi:10.1016/j.aej.2022.07.001.
22. Elsayed, A.; Bastien, C.; Jones, S.; Christensen, J.; Medina, H.; Kassem, H. Investigation of Baffle Configuration Effect on the Performance of Exhaust Mufflers. *Case Studies in Thermal Engineering* **2017**, *10*, 86–94, doi:10.1016/J.CSITE.2017.03.006.